Open Journal of Geology, 2023, 13, 91-106
https://www.scirp.org/journal/ojg
ISSN Online: 2161-7589
ISSN Print: 2161-7570

# Petrochemical Studies of Fouimba and Goma Mounts, Central-West of Cote d'Ivoire: Implication on Petrogenesis Tectonic Setting

**Allialy Marc Ephrem[1*], Siogbo Davy Bedel[2], Kouadio Fossou Jean Luc[1], Houssou N'guessan Nestor[1], Kouassi Brice Rolland[1], Konan Félix Oufouet[1], Diakité Sekou[1]**

[1]Laboratoire GRME, UFR STRM, University Félix Houphouët-Boigny de Cocody Abidjan, Abidjan, Côte d'Ivoire
[2]DGMG, Ministère des Mines de Côte d'Ivoire, Abidjan, Côte d'Ivoire
Email: *marcephremallialy7@gmail.com

**How to cite this paper:** Ephrem, A.M., Bedel, S.D., Kouadio Fossou, J.L. Nestor, H.N., Rolland, K.B., Oufouet, K.F. and Sekou, D. (2023) Petrochemical Studies of Fouimba and Goma Mounts, Central-West of Cote d'Ivoire: Implication on Petrogenesis Tectonic Setting. *Open Journal of Geology*, **13**, 91-106.
https://doi.org/10.4236/ojg.2023.132005

**Received:** December 31, 2022
**Accepted:** February 6, 2023
**Published:** February 9, 2023



## Abstract

Petrogeochemical analysis of mafic rocks of Fouimba and Goma Mount in the Séguéla region (central-western Côte d'Ivoire) is the subject of this study. This analysis combines remote sensing, geophysics, petrography and geochemistry, in order to determine the major characteristics of the mafic formations in the said area, and above all to participate in the detailed mapping of all the Ivorian terrains. The mafic formations encountered in this region are essentially metatonalites to metadiorites, amphibolites, amphibole bearing pyroxenites and porphyry basalts. Chemical analysis indicates that these mafic formations are tonalitic to monzonitic. They are thought to have derived from mantle depleted magmas.

## Keywords

Petrography, Geochemistry, Mount Fouimba and Goma, Seguela, Côte d'Ivoire

## 1. Introduction

Known for its diamond fields fed by kimberlite and lamprophyre dykes, the Séguéla area, located in the central-western part of Côte d'Ivoire, has a certain number of structural, stratigraphic, lithological, magmatic and metamorphic features in its greenstone belts, which at first glance seem to favour the development of significant mineral concentrations.

These numerous particular features have recently attracted the attention of major mining companies, which have acquired a mining exploration permit covering an area of 350 km$^2$ and including the two main mountains in the said zone, namely Mounts GOMA and FOUIMBA. Furthermore, it is clear that Côte d'Ivoire does not yet have detailed geological maps covering the entire country, which would enable all the above-mentioned features to be understood, as few detailed studies have been carried out. It is therefore clear that the establishment of a detailed geological map of the Ivorian terrain is more than necessary. It is therefore in this spirit of necessity that the present study aims to highlight, in a detailed manner, all the petro-structural characteristics of the geological formations in the Seguela area, by means of a 1:50,000 scale map.

## 2. Study Framework

### 2.1. Geographic Location

The town of Seguela is located in the centre-west of Côte d'Ivoire, between longitudes 6˚30'00"W and 7˚00'00"W and latitudes 7˚45'00"N and 8˚15'00"N, with an average altitude of 350 m above sea level. Séguéla is 516 km from Abidjan, the economic capital, and is above all the capital of the Worodougou region, covering an area of 11,427 $km^2$ (**Figure 1**).

### 2.2. Geologie of Man Shield and Study Area

The West African Craton (WAC) is, according to [1]; subdivided into three distinct zones (**Figure 2**): Reguibat Ridge northern part formed by Archean formations (3.0 - 2.7 Ga) separated from Paleoproterozoic formations (~2 Ga) Zednes Fault (a northern extension of the Sassandra Fault), and outcropping in Algeria, Morocco and Mauritania. Man or Leo ridge in the southern part formed Archean series of Liberian Shield, and Paleoproterozoic (Birimian) formations of Baoulé-Mossi Domain covering Ghana, Côte d'Ivoire, Guinea, southern Mali, Burkina Faso, and western Niger. Liberian basement and Birimian series are separated by an Archean-Proterozoic transition zone [2], corresponding to a large complex fault: Sassandra submeridian fault [1] [3]. In an intermediate position between the two ridges are two buttonholes, including the Kayes buttonhole in western Mali and the Kenieba-Kédougou buttonhole on either side of Senegal-Malian border. These buttonholes are formed exclusively by Birimian series.

Ivorian Precambrian basement is a characteristic part of the Man Ridge and is essentially composed of a western Archean domain and an eastern Proterozoic domain. Archean-Proterozoic transition of the Ivory Coast is, according to [1] [3], materialised by a large complex fault called Sassandra Submeridian Fault, with an N-S to NNW-SSE orientation. [4] [5] subdivide this transition zone into three sub-domains, including the Boundiali domain or Northern domain, located north of parallel 9˚; Séguéla-Vavoua domain or Central domain, located between parallels 7˚ and 9˚, in which the present study area is located; and SASCA domain or Southern domain, which extends from parallel 7˚N, to Atlantic coast.

The present study area is based on a thread-like trench called Séguéla-Vavoua, oriented N-S, and the geological formations encountered there are essentially composed of volcano-sedimentary units (greenstone belt) generally oriented N-S to NE-SW. These are essentially, metagranites, metamonzonites, biotite and/or hornblende metagranodiorites, gabbros and metagabbros, metadiorites, amphibolites lamprophyres, tonalites, and biotite granites (**Figure 3**).

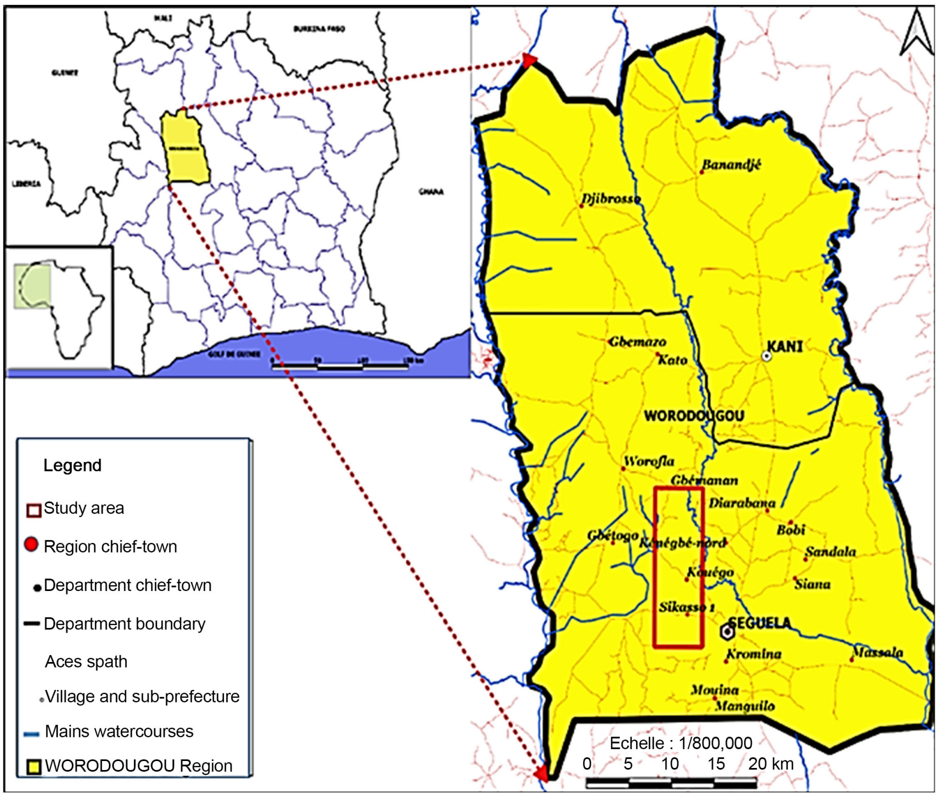


**Figure 1.** Location map of Séguéla area (Administrative map of Cote d'Ivoire, 2013).

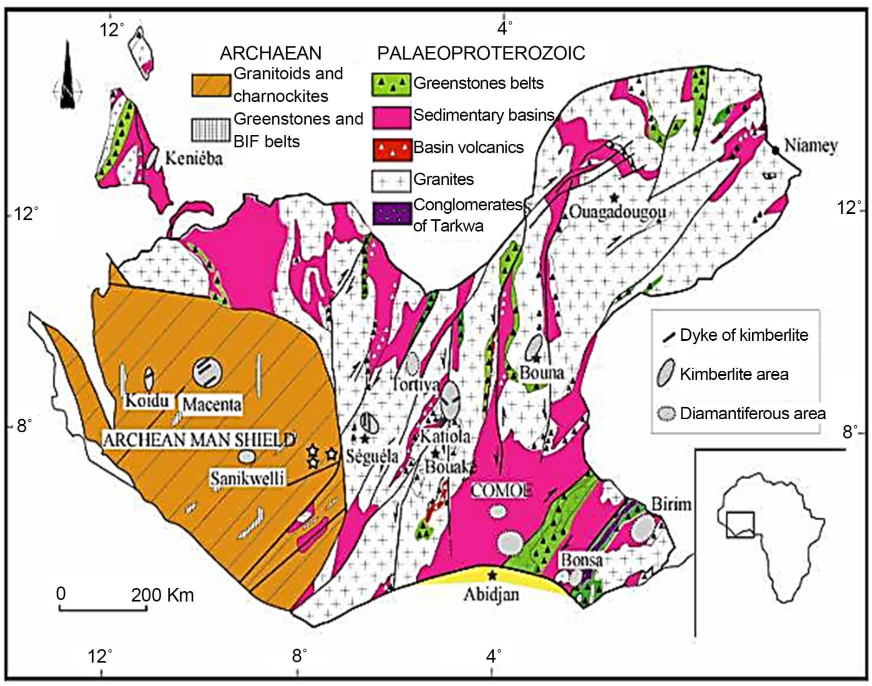


**Figure 2.** Geologic map of the West African craton (Berger *et al.*, 2013 modified).

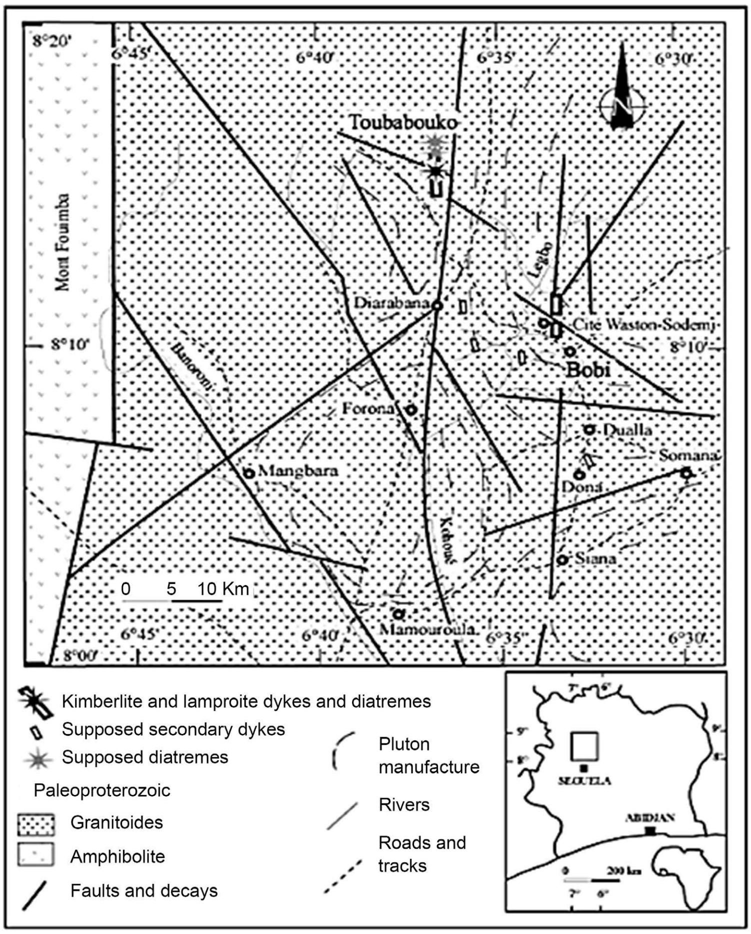


**Figure 3.** Séguéla area geological map: 1/200,000 (Tagini 1972, modified).

## 3. Analytical Methods

• **Major and REE Elements Analysis**

The geochemical data were realized within the analytical laboratory of the CRPG (Nancy, France). Major oxide analyses were obtained using emission spectroscopy on ICP-AES whereas trace-element geochemistry was determined by mass spectroscopy on ICP-MS. Results for both major and trace elements are given in **Table 1**. Samples were chipped and cleaned in acid before being crushed and powdered. Powders were mixed by coning several times to ensure homogeneity. 300 mg of the powdered sample were considered for determination of loss on ignition by living the samples in a muffle furnace at 1000˚C for 12 hours. For preparation of glass fusion discs, the sample was mixed with lithium tetraborate (LiBO3) and the mixture was heated in a furnace to 1050˚C and cast in carbon dies to form the discs.

Major elements, together with V, Cr, Ni, Zn, Ga, Rb, Sr, Y, Zr, Nb, Ba, La, Ce, Pb, and Th were analyzed on the prepared discs by X-Ray fluorescence (XFR) spectrometer at the Centre de Recherche Pétrographique et Géochimique de Nancy (France) using spectrometer ICP-AES Jobin Yvon JY70 for major elements (Si, Al, Fe total, Mn, Mg, Ca, Na, K, P, Ti).

## 4. Results

### 4.1. Tele-Analytical Data

Two main types of remote sensing data have been used in this paper. These include satellite imagery data and aeromagnetic data.

- **Major and REE Elements Analysis**

The processing of the satellite images and the systematic analysis of the lineaments obtained allowed us to identify 4 major directions of the structures, of which the main one is oriented NNE-SW, the secondary direction NE-SW, the tertiary one is oriented WNW-SE and the quaternary one is oriented NNW-SSE. In fact, the lineaments between [N0˚- N45˚] constitute about 28.88%; the lineaments between [N46˚- N90˚] constitute about 25.26%; the lineaments between [N90˚- N135˚] constitute about 23.64%; and the lineaments between [N135˚-N180˚] constitute about 22.22%. These so-called major lineament directions are distributed in a very homogeneous manner over the entire study area, and for the most part do not occupy any preferential quadrants in the study area (**Figure 4**).

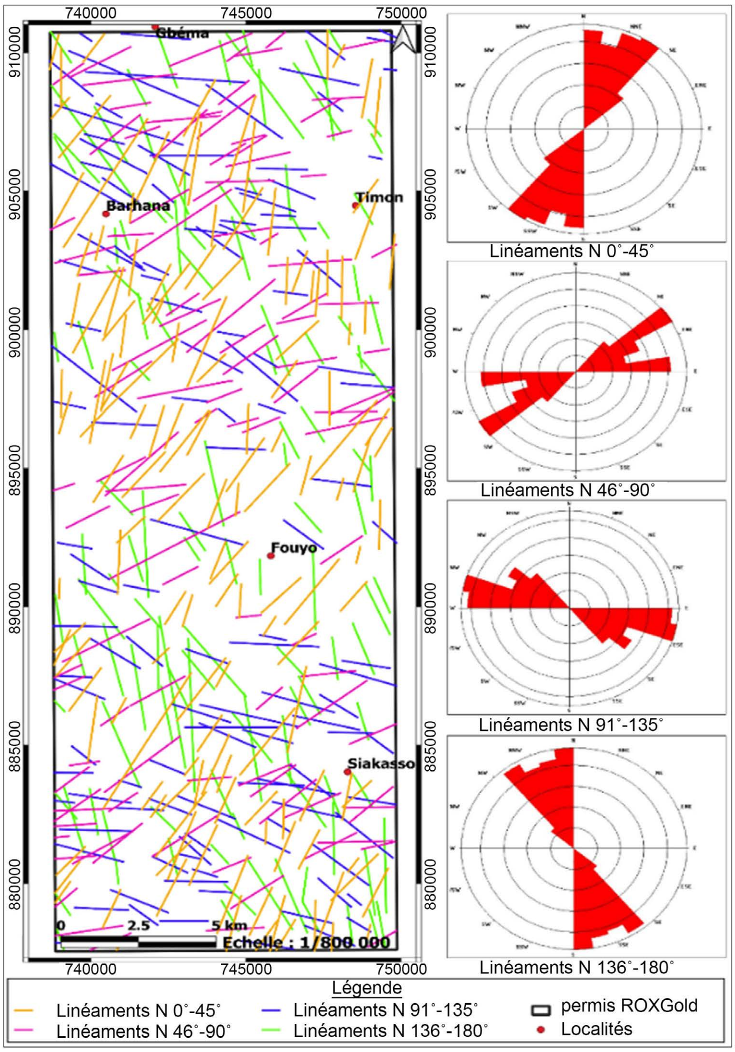


**Figure 4.** Thematic map of the lineament (481 lineaments).

- **Geophysic**
  - **Map of the Reduced Magnetic Field at the Equator**

The analysis and interpretation of the map of the reduced field at the equator made it possible to identify the major structural features of the study area (**Figure 5**).

## 4.2. Lithology

The geological survey carried out in the study area revealed a range of rock outcrops from which samples were taken for a more detailed petrographic study. Metamorphic formations of the surveyed area are essentially composed of metatonalites, amphibolites and amphibolo-pyroxenites, located mainly on Mount Fouimba.

- **Metatonalites**

The Metatonalite has been encountered at Sifié (North-West), Béna and Forona (North-East). It is mesocratic with a grainy oriented texture. The Bena sample shows a grouping of light minerals (quartz and feldspars) forming leucozomes and dark minerals (biotites and amphiboles) forming melanozomes, materialising the foliation in the rock. Microscopic examination of this rock has enabled us to identify its mineral paragenesis, which is as follows (**Figure 6**).

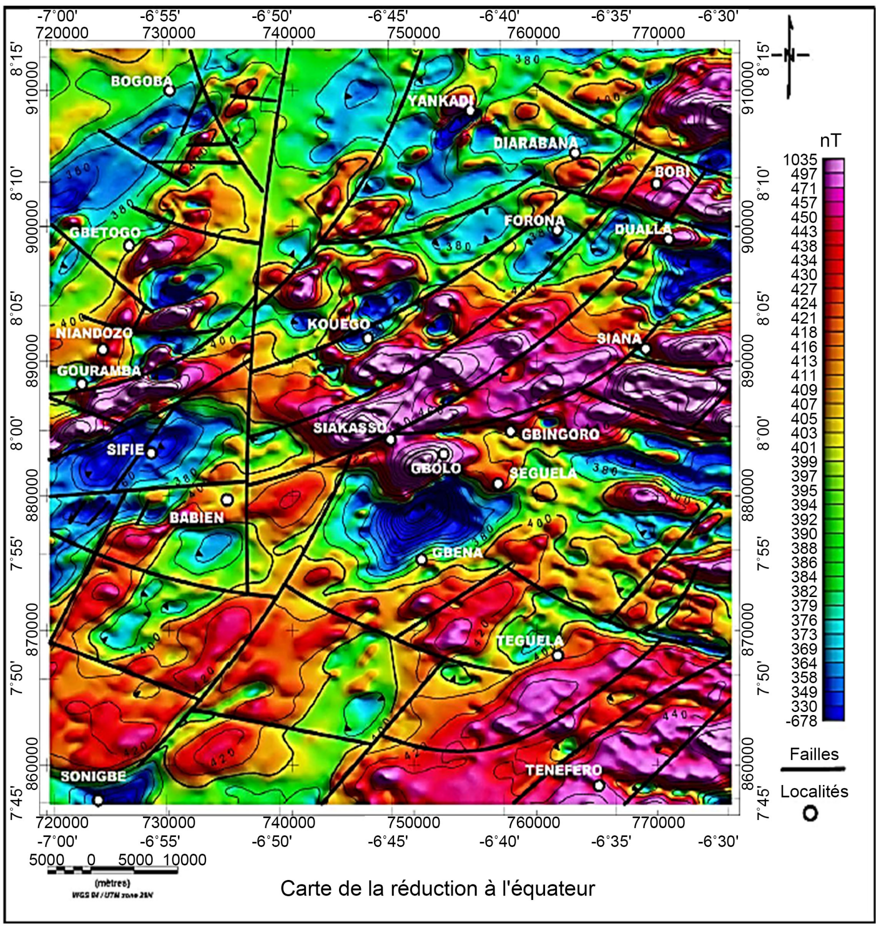


**Figure 5.** Map of the reduction at the equator coupled with major structures of the study area.

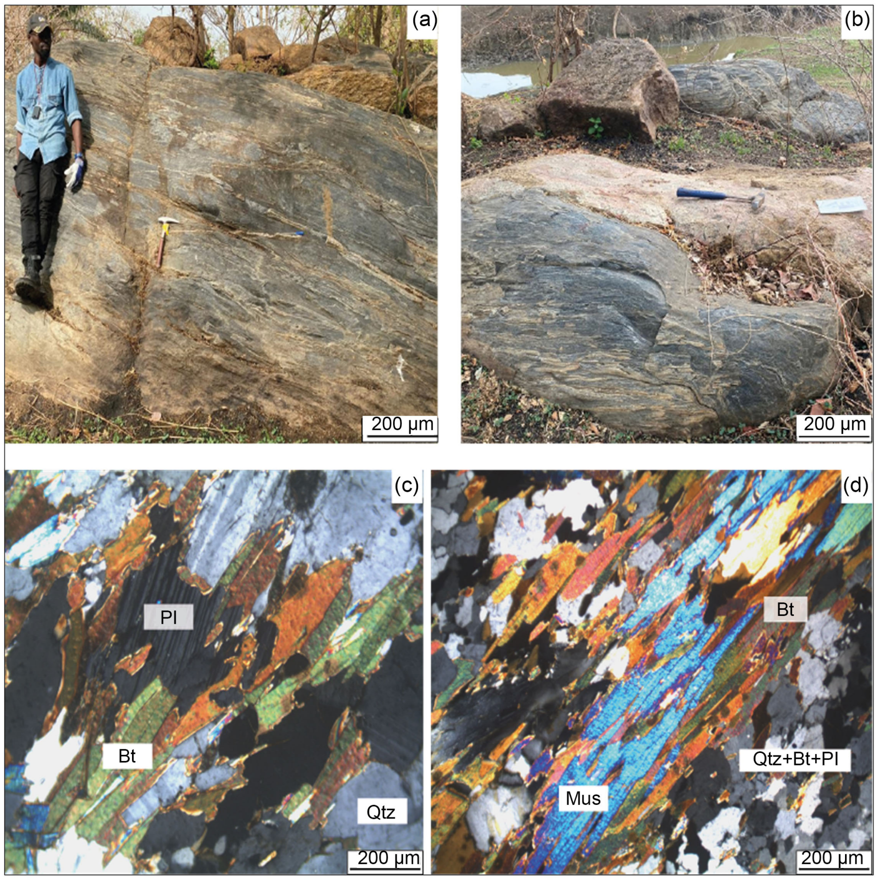


**Figure 6.** Macroscopic and microscopic aspects of metatonalites. (a): outcrop of metatonalite, (b): outcrop of metatonalite with a 1.6 m wide pegmatite vein, (c): oriented biotite rods associated with plagioclase and quartz, (d): extensive stretching and orientation of biotite and muscovite minerals associated with plagioclase and quartz. Bt: Biotite, Pl: Plagioclase, Qtz: Quartz, Mus: muscovite.

- **Amphibolites**

They were observed mainly in the Fouimba and Goma mountains, more precisely in the centre of the study area. These formations are hard and compact, moderately to slightly altered, greenish in colour and fine to medium grained. Under the microscope, these rocks have a grano-nematoblastic texture with the following mineralogy (Figure 7).

- **Amphibolo-pyroxenites**

The outcrops encountered are generally in the form of blocks. They have been found mainly in Monts Fouimba and Goma. They are massive, very dense and greenish in colour. Microscopically, they generally have a granonematoblastic texture with the following mineralogical composition (Figure 8).

### 4.3. Geochemistry

#### 4.3.1. Classification and Geochemical Nature of Fouimba and Goma Greenstones

Chemical compositions of samples from basic formations are plotted into rocks classification diagrams. Inserted in the $Na_2O + K_2O$ (wt%) versus $SiO_2$ (wt%)

diagram of [6], all the basic formations of the study area show mostly gabbroic and dioritic compositions (**Figure 9**) and (**Table 1**). A minority of the basic formations are tonalitic to monzonitic.

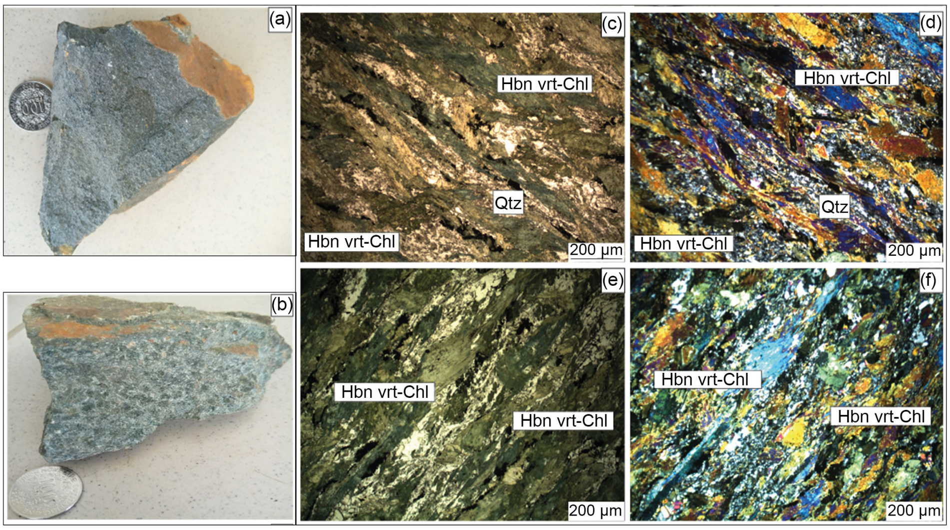


**Figure 7.** Macroscopic and microscopic aspects of amphibolites. (a): macroscopic sample of the medium-grained amphibolites, (b): macroscopic sample of the porphyritic amphibolites, (c): highly oriented green hornblende minerals in unanalysed polarised light (LPNA), (d): highly oriented green hornblende minerals in analysed polarised light (LPA), (e): green hornblende and quartz mineral assemblage (LPNA), (f): green hornblende and quartz mineral assemblage (LPA), Hnb-vrt: green hornblende, Qtz: quartz, Chl: chlorite.

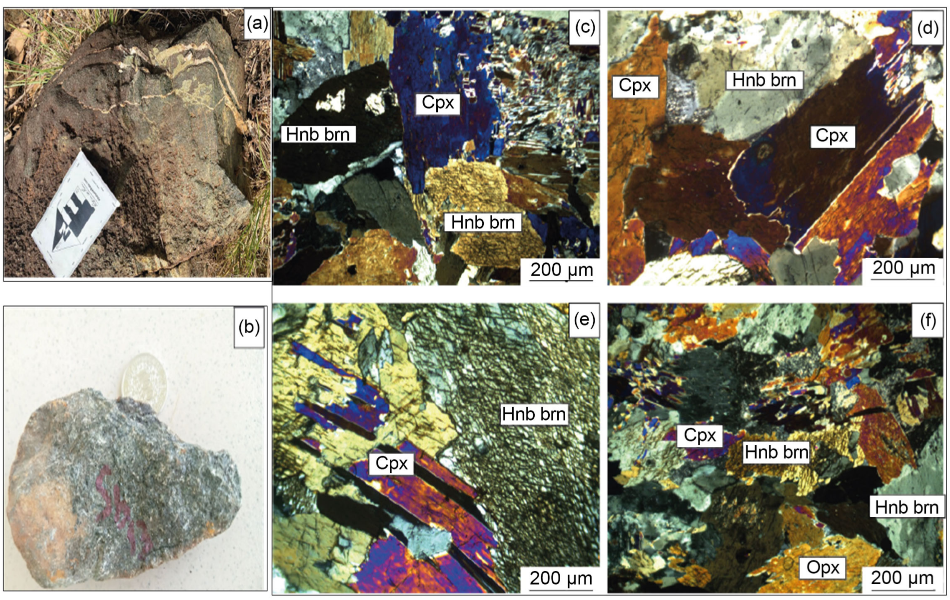


**Figure 8.** Macroscopic and microscopic aspects of amphibolo-pyroxenites. (a): macroscopic sample of amphibolo-pyroxenites, (b): macroscopic sample of Amphibolo-pyroxenites, (c): cumulative texture of amphibolo-pyroxenite in polarised light (LPNA), (d): highly oriented clinopyroxene in analysed polarised light (LPA), (e): green hornblende and clinopyroxene assemblage (LPNA), (f): green hornblende and orthopyroxene minerals assemblage (LPA), Hnb-brn: brown hornblende, CPX: Clinopyroxene, OPX: orthpyroxene.

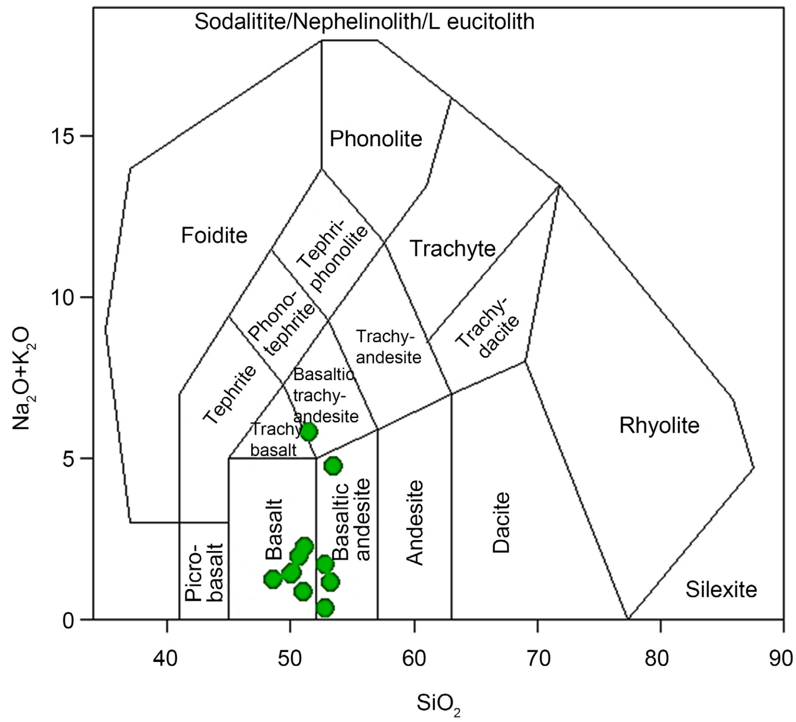


**Figure 9.** Diagram TAS ($Na_2O + K_2O$) versus $SiO_2$ (Cox *et al.*, 1979) applied to mafic formations.

**Table 1.** Major elements composition in Séguéla greenstones.

| Sample | SB4 | SB7 | SB11B | SB13 | SB17A | SB17B | SB18A | SB18B | SB19A | SB19B | SB24B |
|---|---|---|---|---|---|---|---|---|---|---|---|
| $SiO_2$ | 52.38 | 47.66 | 53.37 | 53.12 | 49.92 | 50.27 | 50.51 | 49.1 | 49.05 | 51.98 | 51.14 |
| $Al_2O_3$ | 13.12 | 15.35 | 15.04 | 5.25 | 13.44 | 14.49 | 14.66 | 14.94 | 14.89 | 13.66 | 14.6 |
| $Fe_2O_3$ | 12.82 | 13.32 | 10.79 | 10.87 | 15.61 | 11.62 | 11.4 | 13.15 | 10.77 | 11.46 | 10.67 |
| CaO | 14.45 | 11.4 | 9.16 | 12.77 | 11.08 | 11.94 | 11.12 | 9.86 | 10.96 | 9.83 | 8.13 |
| MgO | 4.65 | 7.67 | 5.53 | 15.81 | 6.61 | 8.34 | 7.67 | 8.12 | 8.15 | 8.84 | 7.44 |
| $Na_2O$ | 0.24 | 1.16 | 3.85 | 0.87 | 1.24 | 0.79 | 2.15 | 1.36 | 1.81 | 1.56 | 3.95 |
| $K_2O$ | 0.06 | 0.03 | 0.86 | 0.27 | 0.12 | 0.04 | 0.07 | 0.05 | 0.06 | 0.08 | 1.8 |
| MnO | 0.13 | 0.19 | 0.17 | 0.25 | 0.23 | 0.16 | 0.17 | 0.17 | 0.17 | 0.18 | 0.22 |
| $TiO_2$ | 1.11 | 1.07 | 0.86 | 0.36 | 1.42 | 0.84 | 0.97 | 1 | 0.75 | 0.78 | 0.92 |
| $P_2O_5$ | 0.09 | 0.09 | 0.14 | 0.06 | 0.11 | 0.06 | 0.08 | 0.08 | 0.06 | 0.06 | 0.5 |
| $Cr_2O_3$ | 0.03 | 0.03 | 0.02 | 0.08 | 0.02 | 0.04 | 0.03 | 0.03 | 0.03 | 0.05 | 0.03 |
| LOI | 1.19 | 2.92 | 0.6 | 1.41 | 0.73 | 2.24 | 1.77 | 2.65 | 3.41 | 2.23 | 0.66 |
| Total | 100.27 | 100.89 | 100.39 | 101.12 | 100.53 | 100.83 | 100.6 | 100.51 | 100.11 | 100.71 | 100.06 |
| Ba | 26 | 54 | 182 | 110 | 49 | 34 | 32 | 20 | 39 | 22 | 536 |
| Be | <1 | <1 | <1 | <1 | 2 | <1 | <1 | <1 | <1 | <1 | 3 |
| Co | 40.4 | 57.9 | 40.6 | 75.1 | 53.7 | 45.8 | 42.3 | 56.8 | 46 | 43.5 | 41.6 |
| Cs | 0.3 | <0.1 | 0.7 | 0.7 | <0.1 | <0.1 | <0.1 | 0.1 | <0.1 | <0.1 | 1.1 |
| Ga | 22.9 | 15.8 | 16.8 | 7.8 | 16 | 13.6 | 14 | 13.7 | 12.6 | 12 | 15.7 |

**Continued**

| | | | | | | | | | | | |
|---|---|---|---|---|---|---|---|---|---|---|---|
| Hf | 1.7 | 1.6 | 2.5 | 1.7 | 2.1 | 1.4 | 1.5 | 1.7 | 1.3 | 1.4 | 5.9 |
| Nb | 2.7 | 2.6 | 3.2 | 1.8 | 3.2 | 2 | 1.9 | 2.3 | 1.7 | 1.8 | 9.4 |
| Rb | 1.8 | 0.4 | 29.7 | 7.6 | 1.4 | 0.4 | 0.4 | 0.2 | 0.3 | 0.4 | 68.5 |
| Sn | <1 | <1 | <1 | <1 | <1 | <1 | <1 | <1 | <1 | <1 | 3 |
| Sr | 111.5 | 130.9 | 356.6 | 96.2 | 95.7 | 75.6 | 103.5 | 88.1 | 89.8 | 68.6 | 403.1 |
| Ta | 0.2 | 0.2 | 0.2 | 0.1 | 0.2 | 0.1 | 0.1 | 0.1 | 0.1 | 0.1 | 0.5 |
| Th | 0.4 | 0.3 | 3.6 | 2.4 | 0.5 | 0.3 | 0.2 | <0.2 | 0.2 | 0.3 | 6.4 |
| U | 0.1 | <0.1 | 1 | 0.5 | <0.1 | <0.1 | <0.1 | <0.1 | <0.1 | <0.1 | 2 |
| V | 290 | 285 | 212 | 161 | 371 | 255 | 268 | 269 | 231 | 219 | 216 |
| W | 0.5 | 0.5 | <0.5 | 3.5 | 0.5 | 0.7 | <0.5 | <0.5 | <0.5 | <0.5 | <0.5 |
| Zr | 60.6 | 59.7 | 91.1 | 50.3 | 77.3 | 48.8 | 50.6 | 51.6 | 43.6 | 46.1 | 214.8 |
| Y | 47.4 | 21.9 | 17.4 | 16.8 | 28.2 | 19 | 18.2 | 18.7 | 17.4 | 16.8 | 22.8 |
| La | 101.7 | 4.3 | 19.8 | 10.1 | 6.8 | 3.8 | 2.9 | 3 | 3.9 | 3.4 | 33 |
| Ce | 16.2 | 9.8 | 47.5 | 21.4 | 12.5 | 8.3 | 7.4 | 7.4 | 7.6 | 8 | 75.8 |
| Pr | 30.44 | 1.44 | 5.41 | 3.21 | 2.06 | 1.26 | 1.17 | 1.15 | 1.26 | 1.18 | 10.51 |
| Nd | 112.4 | 6.9 | 21.4 | 14.8 | 10.4 | 6.2 | 6.6 | 6.1 | 5.9 | 6.1 | 44.3 |
| Sm | 19.03 | 2.22 | 3.95 | 3.73 | 3.15 | 1.91 | 1.99 | 1.94 | 1.79 | 1.81 | 8.25 |
| Eu | 5 | 0.85 | 1.22 | 0.84 | 1.17 | 0.69 | 0.81 | 0.72 | 0.7 | 0.72 | 2.27 |
| Gd | 13.74 | 3.19 | 3.47 | 3.68 | 4.24 | 2.53 | 2.72 | 2.77 | 2.49 | 2.45 | 6.89 |
| Tb | 2.03 | 0.58 | 0.53 | 0.57 | 0.75 | 0.47 | 0.5 | 0.51 | 0.46 | 0.43 | 0.87 |
| Dy | 10.45 | 3.71 | 3.12 | 3.23 | 4.81 | 3.19 | 3.14 | 3.2 | 3.01 | 2.88 | 4.59 |
| Ho | 1.97 | 0.84 | 0.66 | 0.65 | 1.15 | 0.65 | 0.72 | 0.72 | 0.66 | 0.61 | 0.81 |
| Er | 5.07 | 2.5 | 1.96 | 1.86 | 3.17 | 2.12 | 2.06 | 2.14 | 2.02 | 1.89 | 2.33 |
| Tm | 0.72 | 0.37 | 0.28 | 0.26 | 0.45 | 0.29 | 0.29 | 0.32 | 0.28 | 0.28 | 0.31 |
| Yb | 4.44 | 2.33 | 1.87 | 1.6 | 3.01 | 1.91 | 1.88 | 2.09 | 1.89 | 1.84 | 2.07 |
| Lu | 0.61 | 0.37 | 0.3 | 0.25 | 0.45 | 0.3 | 0.3 | 0.31 | 0.29 | 0.28 | 0.3 |
| Mo | 0.1 | 0.3 | 0.4 | <0.1 | 0.3 | 0.2 | 0.3 | 0.2 | 0.1 | <0.1 | 0.4 |
| Cu | 37.1 | 126.2 | 57.6 | 67.4 | 138.3 | 83.4 | 115.7 | 122.6 | 112.8 | 81.1 | 13.8 |
| Pb | 0.7 | 0.2 | 2.6 | 0.8 | 0.4 | 0.3 | 0.2 | 0.3 | 0.1 | 0.2 | 3 |
| Zn | 18 | 54 | 41 | 14 | 32 | 39 | 35 | 53 | 38 | 40 | 75 |
| Ni | 21 | 141.9 | 33 | 100.7 | 38 | 61.2 | 80.2 | 144.3 | 92.7 | 64.6 | 49.6 |

#### 4.3.2. Traces Elements Geochemistry

The MgO vs. Harker Oxides diagrams shows a clustered distribution of representative points of the mafic rock samples from the study area. This distribution indicates positive correlations between MgO and the majority of elements including $Al_2O_3$, $SiO_2$, $Fe_2O_3$, CaO, $TiO_2$, $P_2O_5$. Negative correlations exist with $SiO_2$ but it is less clear with $Na_2O$ which seems to be negative. In detail, the mafic formations of Seguela area show a similar composition (**Figure 10**).

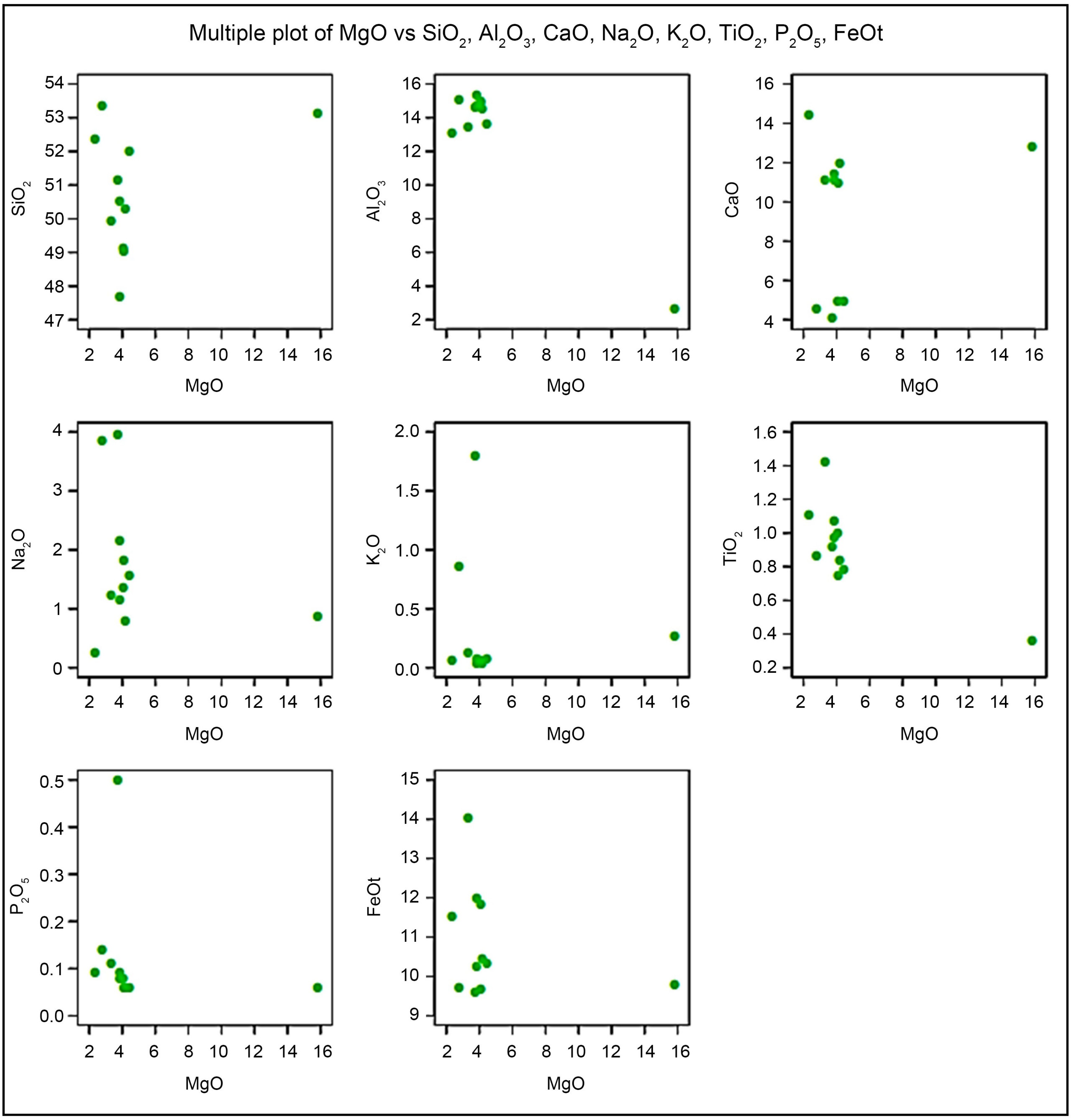


**Figure 10.** Distribution of major elements vs MgO about mafic formations in Mount Fouimba-Séguéla area.

The Seguela kimberlites have steep REE [7] patterns (**Figure 11**) with (La/Yb)n = 2 - 23 which is typical of MORB (**Table 2**). Comparative element abundance plots [8] normalized against primitive mantle values (**Figure 12**) show marked large-ion with pronounced positive Nb, Nd, and Sm anomalies, and negative K, Sr, P, Hf, and Zr lithophile element (LILE) and LREE enrichments (X > 100 times primitive mantle abundance) anomalies. These are all features previously documented for MORB and Primitive mantle [9]. These elemental abundance patterns indicate that amphibolites have a close affinity with MORB (**Figure 13**).

Incompatibles elements contents are similar to those of N-MORB, intraplate basaltic rocks (e.g., non-DUPAL OIBs) [10] (**Figure 14**).

#### 4.3.3. Tectonic Setting

[11] diagram indicates that most of mafic formations in the study area would have formed predominantly in mantle depleted context (**Figure 15**).

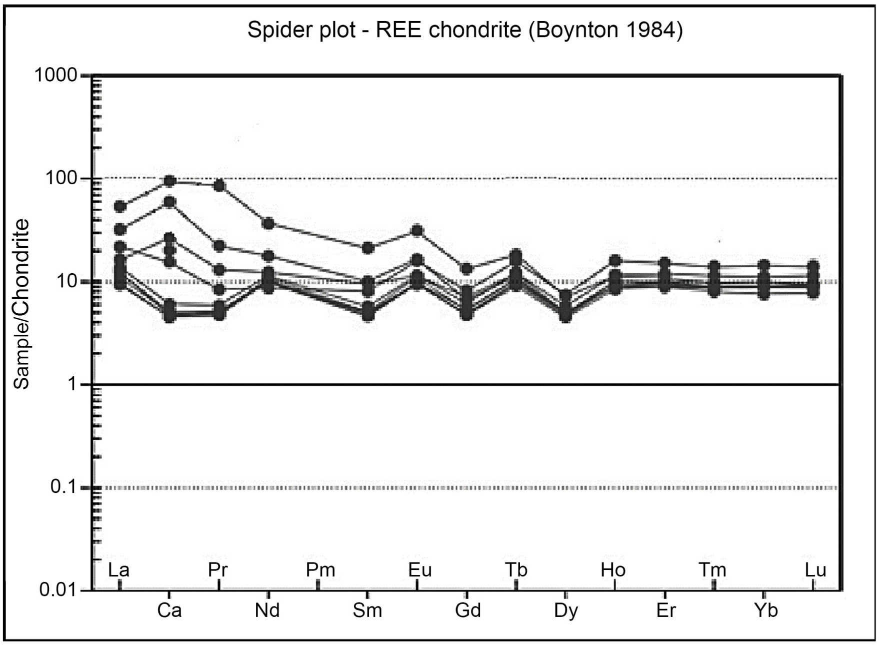


**Figure 11.** Selected chondrite normalised REE patterns for Seguela greenstones belt samples (Boynton, 1984).

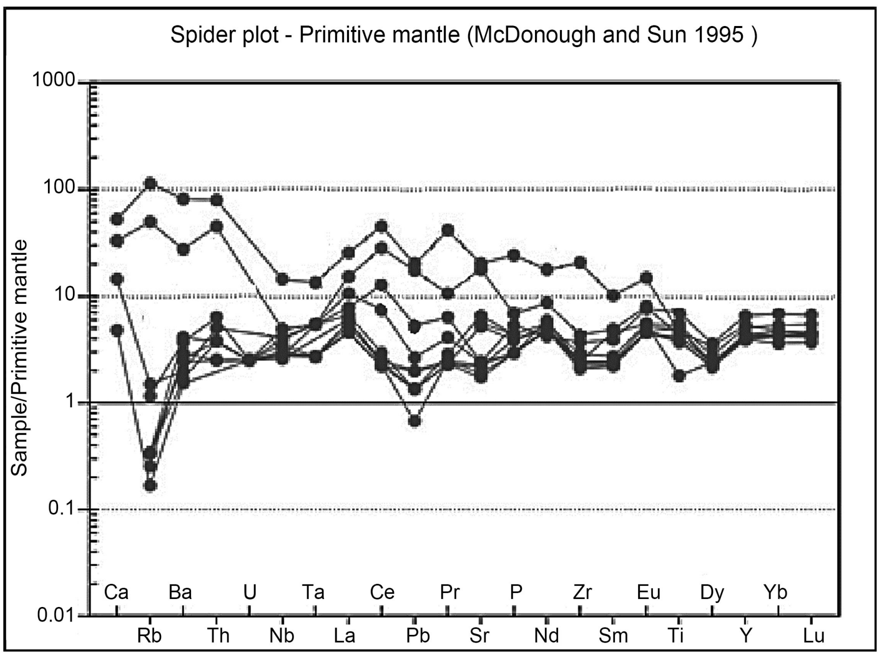


**Figure 12.** Average Seguela greestones samples element abundance patterns normalized against primitive mantle (McDounough and Sun, 1995).

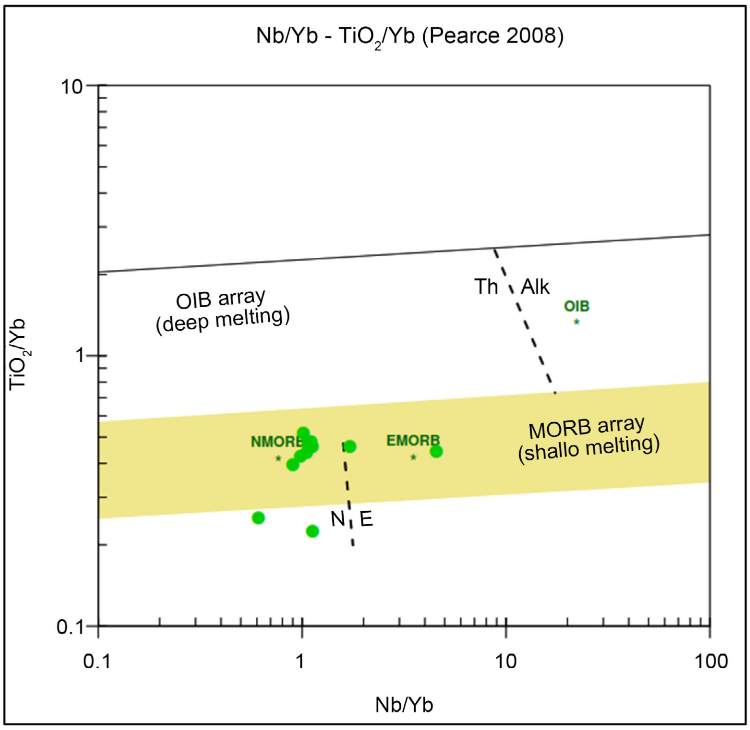


**Figure 13.** Diagram($TiO_2$/Yb) versus (Nb/Yb) from Pearce (2008), applied to mafic formations. NMORB: N-type mid-oceanic ridge basalt; EMORB: E-type midoceanic ridge basalt; OIB: oceanic island basalt; Th: tholeitic; Alk: alkaline.

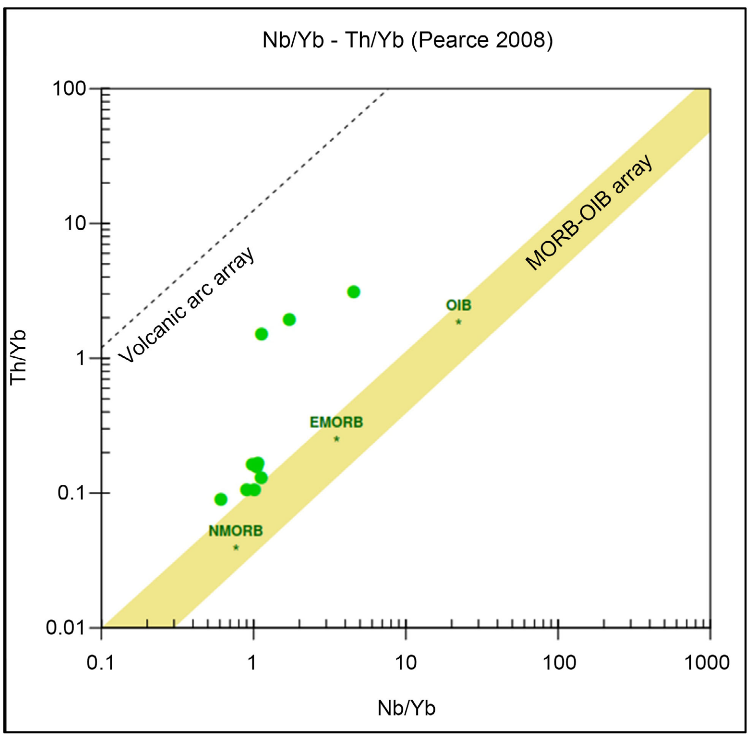


**Figure 14.** Diagram(Nb /Yb) versus (Th/Yb) from Pearce (2008), applied to mafic forma NMORB: N-type mid-oceanic ridge basalt; EMORB: E-type mid-oceanic ridge basalt. OIB: oceanic island basalt

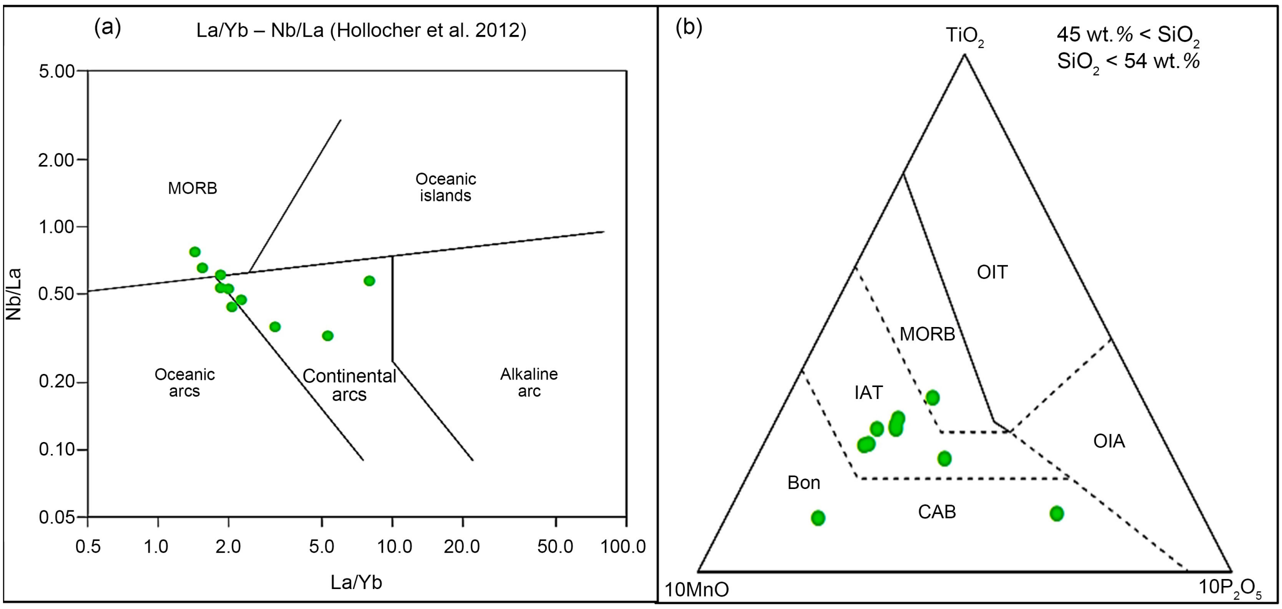


**Figure 15.** (a): Binary diagram (Nb/La) versus (La/Ya); from Hollocher *et al.* (2012) aplied to mafic formations, (b): Ternary diagram 10 Mno-$TiO_{2\text{-}10}$. $P_2O_5$ showing seguela grenstones affinity after Mullen (1983).

**Table 2.** Fouimba and Goma (Séguéla) greenstones traces elements ratios.

| Sample | SB4 | SB7 | SB11B | SB13 | SB17A | SB17B | SB18A | SB18B | SB19A | SB19B | SB24B |
|---|---|---|---|---|---|---|---|---|---|---|---|
| La/Yb | 22.91 | 1.85 | 10.59 | 6.31 | 2.26 | 1.99 | 1.54 | 1.44 | 2.06 | 1.85 | 15.94 |
| Nb/La | 0.03 | 0.6 | 0.16 | 0.18 | 0.47 | 0.53 | 0.66 | 0.77 | 0.44 | 0.53 | 0.28 |
| Ce/Sr | 0.15 | 0.07 | 0.13 | 0.22 | 0.13 | 0.11 | 0.07 | 0.08 | 0.08 | 0.12 | 0.19 |
| Zr/Hf | 35.65 | 37.31 | 36.44 | 29.59 | 36.81 | 34.86 | 33.73 | 30.35 | 33.54 | 32.93 | 36.41 |
| Nb/Ta | 13.5 | 13 | 16 | 18 | 16 | 20 | 19 | 23 | 17 | 18 | 18.8 |
| Nb/Zr | 0.04 | 0.04 | 0.04 | 0.04 | 0.04 | 0.04 | 0.04 | 0.04 | 0.04 | 0.04 | 0.04 |
| Zr/Nb | 22.44 | 22.96 | 28.47 | 27.94 | 24.16 | 24.4 | 26.63 | 22.43 | 25.65 | 25.61 | 22.85 |
| Ce/Y | 0.34 | 0.45 | 2.73 | 1.27 | 0.44 | 0.44 | 0.41 | 0.4 | 0.44 | 0.48 | 3.32 |

## 5. Discussion

The transition zone (Archean-Proterozoic) of Côte d'Ivoire is, according to studies by [12]; [4] subdivided into three domains: the Northern domain (Boundiali domain), the Central domain (Séguéla-Vavoua domain) and the Southern domain (SASCA domain). Compared to the other domains of the transition zone, the present study area (Séguéla-Vavoua domain) shows many similarities but above all important differences:

In the northern domain of the transition zone, [12]; [4] describe intrusive granitic massifs and amphibolites whose characteristics are similar to those described in the present area. In the southern part of the transition zone, [12]; [4] identify as a particular feature the coexistence of high-grade formations considered as Archean (anatexes, tonalitic orthogneisses more or less migmatitic.) and low-grade formations considered as Birimian (intrusive leucogranites, intrusive granodiorites, micaschists…). [13] identifies three major lithological units in this area, and more precisely at Bliéron (Grand-Béréby), which are not all identified in the Séguéla. Metabasites are characterised by metatonalites, gabbros, basalts and amphibolites. Low Nb/La and Ce/Sr ratios observed in the Seguela amphibolites show that also indicates protholite is not sediment recycling [14]. In this case greenstones alteration has caused elevated occupy of the MORB fields (**Figure 13**, **Figure 14**). The presence of lower content of Zr (<50 ppm), and higher Zr/Nb ratio (**Table 2**) varying from 22 to 28, support their MORB nature. A small amount of partial melting of a spinel-garnet-lherzolite source cannot produce lower La/Yb ratios. Lower La/Yb and significantly low Rb, Ba, and Nb represent higher degrees of partial melting.

Seguela ampibolites show relatively Low Rb, Ba, Nb and La/Yb ratios compared with MORB (N-MORB, E-MORB and OIB). Amphibolites, derived from relatively higher degrees of partial melting. Seguela kimberlites have high Zr/Nb ratio and low La/Yb ratios. Conventional interpretation indicates decreasing La/Yb ratios represent an increasing amount of partial melting. Thus it is evident that the Seguela amphibolites are formed by higher degrees of partial melting of the mantle source relative to MORB (N-MORB &e-MORB). The Ce/Y and Zr/Nb ratios are commonly used to infer the degrees of melting involved in the production of basaltic rocks from a peridotitic source. Rocks that derive from a similar source tend to show a decrease in Ce/Y with increasing Zr/Nb. Seguela amphibolites show that Ce/Y decreases with increasing Zr/Nb indicating that they are derived from the same source. The La/Yb ratios (1 to 23) of Seguela amphibolites are similar to MORB [11]. However, the lower concentrations of Rb, Ba and K in Seguela rocks may be indicative of no residual phlogopite in the source.

## 6. Conclusions

In view of all this, we can conclude that Seguela mafic formations are components of amphibolites, and amphibolo-pyroxenites, metaonalite, mostly affected by greenschist to amphibolite facies metamorphism. Significant hydrothermalism and weathering are marked on every rock. Hydrothermal weathering is proved by carbonation, sericitisation, chloritisation, epidotization, silicification and sulphudation.

Seguela mafic rocks derived from partial melting. Enrichment in incompatibles elements fractionated REE patterns and high volatile content pointed toward a primitive mantle origin. They have on average higher abundances of LILE and LREE. Geochemistry signatures are characterized by (La/Yb)n, Th/Yb, Zr/Nb, and Ta/Yb ratios which are similar to other Ivory Coast, and west African mafic rocks. Ratios reflect subduction zone environment, tholeitic magmas and MORB, IAT, OIB geochemical signatures related to mantle depleted magmas sources.

## Conflicts of Interest

The authors declare no conflicts of interest regarding the publication of this paper.

## References

[1] Bessoles, B. (1977) Geology of Africa. The West African Craton. Mémoire du BRGM, Paris, No. 88, 404.

[2] Papon, A. (1973) Geology and Mineralization of South-West Côte d'Ivoire. Mémoire du BRGM, Paris, 284 p.

[3] Caby, R., Delor, C. and Agoh, O. (2000) Lithology, Structure and Metamorphism of the Birimian Formations in the Odienne Area [Ivory Coast]: The Major Role Played by Plutonic Diapirism and Strike-Slip Faulting at the Border of the Man Craton. *Journal of African Earth Sciences*, **30**, 351-374. https://doi.org/10.1016/S0899-5362(00)00024-5

[4] Camil, J. (1995) Significant Influence of the Birimian on the Archaean Domain of the Ivory Coast. Séance Spéc. Soc. Géol. Fr. Session, Geodynamique du Paléoprotérozoïque, Orléans, 17 Nov. 1995, 21.

[5] Kouamelan, A.N. (1996) Geochronology and Geochemistry of the Archean and Proterozoic Formations of the Man Ridge in Ivory Coast, Implication for the Archean-Proterozoic Transition. Mém. Geosciences Rennes, 73, 289.

[6] Middlemost, E.A.K. (1994) Naming Materials in the Magma/Igneous Rock System. *Earth Science Reviews*, **37**, 215-224. https://doi.org/10.1016/0012-8252(94)90029-9

[7] Boynton, W.V. (1984) Geochemistry of the Rare Earth Elements: Meteorite Studies. In: Henderson, P., Ed., *Rare Earth Element Geochemistry*, Elsevier, Amsterdam, 63-114. https://doi.org/10.1016/B978-0-444-42148-7.50008-3

[8] McDonough, W.F. and Sun, S.S. (1995) The Composition of the Earth. *Chemical Geology*, **120**, 223-253. https://doi.org/10.1016/0009-2541(94)00140-4

[9] Meschede, M. (1986) A Method of Discriminating between Different Types of Mid-Ocean Ridge Basalts and Continental Tholeiites with the Nb-1bZr-1bY Diagram. *Chemical Geology*, **56**, 207-218. https://doi.org/10.1016/0009-2541(86)90004-5

[10] Pearce, J.A. (2008) Geochemical Fingerprinting of Oceanic Basalts with Applications to Ophiolite Classification and the Search for Archean Oceanic Crust. *Lithos*, **100**, 14-48. https://doi.org/10.1016/j.lithos.2007.06.016

[11] Hollocher, K., Robinson, P., Walsh, E. and Roberts, D. (2012) Geochemistry of Amphibolite-Facies Volcanics and Gabbros of the Støren Nappe in Extensions West and Southwest of Trondheim, Western Gneiss Region, Norway: A Key to Correlations and Paleotectonic Settings. American *Journal of Science*, **312**, 357-416. https://doi.org/10.2475/04.2012.01

[12] Camil, J. (1984) Petrography, Chronology of the Archaeal Assemblages and Associated Formations of the Man Region (Ivory Coast). Implications for the Geological History of the West African Craton. Ph.D. Thesis, University of Abidjan, Abidjan, 306.

[13] Kouadio, F.J.-L.H. (2017) Petrostructural Study of the Geological Formations of South-wEstern Cote d'Ivoire (Blieron-Grand Bereby Sector): Contribution of Geochemistry and Metamorphism Deformation Couple. Université Félix Houphouët Boigny, Abidjan, 221.

[14] Allialy, M.E. (2006) Petrology and Geochemistry of the Diamondiferous Kimberlites of Séguéla. Doctoral Thesis, University of Cocody, Abidjan, 162.